Electrospinning in Near-Critical CO_2

Zhihao Shen,[†] Bowlin E. Thompson,[‡] and Mark A. McHugh*[,‡]

Philip Morris USA Postgraduate Research Program, 4201 Commerce Road, Richmond, Virginia 23234, and Department of Chemical and Life Science Engineering, Virginia Commonwealth University, Richmond, Virginia 23284

Received September 17, 2006
Revised Manuscript Received October 15, 2006

Several reviews[1,2] describe the electrospinning of polymer solutions to make nanofibers with a desired structure, morphology, and orientation. While electrospinning is a versatile technology, there still remains several refractory polymers that are not amenable to electrospinning due to either an excessively high polymer solution viscosity, which leads to clogging of the spinneret, or the nonvolatile character of the solvent, which is not readily removed from the nascent fiber. Although high-temperature electrospinning might be envisioned to overcome these two limitations, this mode of operation has its own challenges since fiber formation is most easily realized at operating temperatures below the glass transition (T_g) or melting temperatures. The present study describes the application of near-critical CO_2 as an electrospinning processing aid to create fibers with novel morphology readily varied by adjusting the operating pressure and temperature.

There is continued interest for using supercritical fluid (SCF) solvents to process polymers for a variety of market applications.[3−7] A significant limitation of SCF technology for polymer processing is that kilobar pressures are needed to dissolve most polymers in an SCF solvent.[8] However, it is possible to operate at low pressures and realize practical processing advantages by dissolving the SCF solvent into the polymer-rich phase, which lowers solution viscosity by several orders of magnitude, or by extracting low molecular weight solvent from the polymer solution, which facilitates the formation of a dry, solid fiber. The present paper describes the use of near-critical CO_2 to electrospin poly(vinylpyrrolidone) (PVP) from PVP−dichloromethane (DCM) solutions. The formation of PVP fibers is directly related to the DCM−CO_2 phase behavior since the electrospinning operating pressures are well below those needed to dissolve neat PVP in CO_2. In addition, when spinning into a CO_2-rich bath, an open-cell fiber morphology is created with features that correlate with the operating pressure.

Figure 1 shows the pertinent details of the high-pressure, electrospinning apparatus. Premixed polymer solution of 6.5 wt % PVP (Aldrich Chemical, weight-average molecular weight of 1 300 000, T_g = 160 °C, used as received) in DCM (Fisher Chemical, Optima, used as received) is loaded into the mixer, described in detail elsewhere.[9] If desired, CO_2 (Roberts Oxygen Inc., bone dry grade, 99.8% minimum purity, used as received) can be transferred into the mixer gravimetrically using a high-pressure bomb. The polymer solution, mixed by a stir bar activated by an external magnet, is compressed to the desired pressure, measured with a pressure gauge accurate to within ±40 psia, by displacing a movable piston using water pressurized with a pressure generator. The mixer temperature is measured and maintained constant to within ±0.2 °C. While pressurizing the mixer the metering valve is opened and polymer solution is delivered to the needle (0.159 cm o.d. by 0.015 cm i.d.), and the solution flow rate is determined visually using the sapphire windows on the spinning vessel (5.1 cm i.d.). Prior to electrospinning, CO_2 is loaded into the spinning vessel to a desired pressure. A back-pressure regulator (Go Inc., model BP66-1A11QEQ161) on the spinning vessel maintains a constant pressure regardless of the solution flow rate. The target is a glass tube slipped over copper tubing (0.635 cm o.d.) connected to an electrically insulated spark plug (Champion Spark Plug, part no. F121501). A Spellman model CZE1000R high-voltage power supply is used to apply 20 kV to the spark plug. The entire apparatus is at ground potential, except for the spark plug, so the target must be closer to the needle, ~2.5 cm, than the distance to the vessel wall for the polymer solution to be drawn to the target. The diameter and morphology of the fibers are determined by an FEI XL30 environmental scanning electron microscope (ESEM) operating at 10 kV in Hi-Vac mode. Since the polymer−solvent solution is not completely insulating, weak or local charges are expected to exist on the C, H, and Cl atoms in DCM and the N and O atoms in PVP due to the weak acidity of DCM and to PVP−DCM interactions. The local negative charges will be drawn by the electric field to the target, which results in a polymer jet ejecting from the needle and traveling to the target.

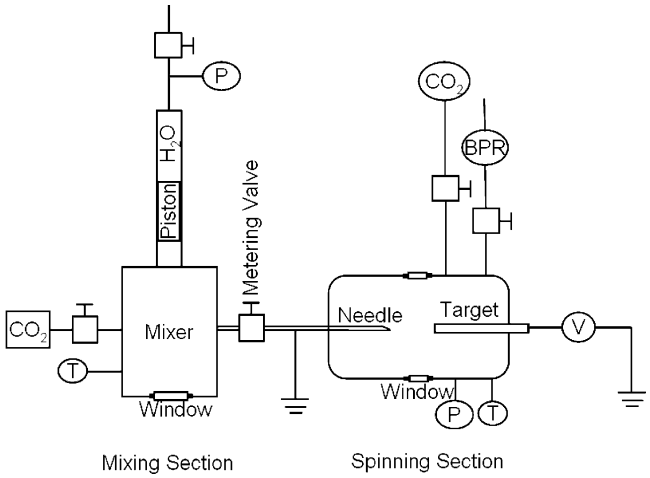

Figure 1. Schematic diagram of the high-pressure electrospinning apparatus used in this study: P = pressure gauge, T = thermocouple, BPR = back-pressure regulator; V = high-voltage dc power supply.

Solid-core PVP fibers are readily produced by spinning PVP−DCM solution at ambient conditions.[10,11] However, it is not possible to create PVP fiber using the high-pressure apparatus at ambient pressures since the needle to target distance is too short for removal of the DCM before the solution hits the target. With the current apparatus high-pressure CO_2 extracts the DCM from the PVP−DCM solution, and the higher the operating pressure, the better the solvent power of CO_2 for DCM. Hence, the formation of PVP fiber is intimately linked with the phase behavior of the DCM in CO_2. Since experimental data for the DCM−CO_2 system are not available at 22 °C, the Peng−Robinson equation of state is used to fit DCM−CO_2 data at 35 °C[12] to determine a reasonable value of the binary interaction parameter, and the 22 °C isotherm is then calculated with the

[†] Philip Morris USA Postgraduate Research Program.
[‡] Virginia Commonwealth University.
* Corresponding author. E-mail: mmchugh@vcu.edu.

10.1021/ma062155i CCC: $33.50
Published on Web 11/09/2006

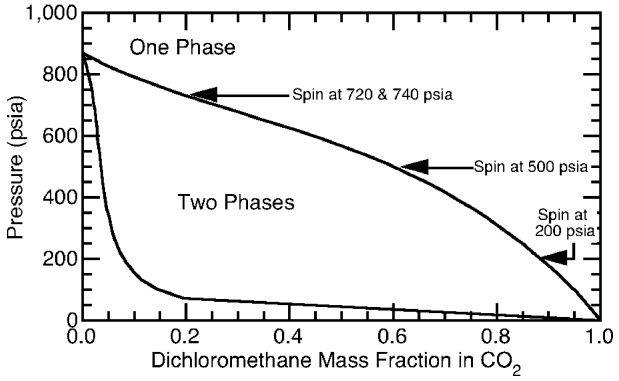

Figure 2. Calculated 22 °C isotherm for the DCM−CO_2 system obtained using the Peng−Robinson equation of state with a binary interaction parameter, 0.050, fit to the 35 °C data of Panayiotou and co-workers.[13]

result shown in Figure 2. Also shown in this figure are the conditions used for electrospinning.

Figure 3 shows the morphology of the electrospun fibers obtained when spinning directly into a bath of CO_2 at 22 °C. For all of these spinning experiments, the voltage was set at 20 kV and approximately the same flow rate is used. The PVP fibers at 200 psia exhibit a solid-core structure similar to that found by spinning PVP−DCM solution at ambient conditions.[11] Note the fibers spun at 500, 720, and 740 psia exhibit a porous internal structure with a coherent external skin. The fiber diameters are on the order of 20−30 μm likely due to the short needle to target distance for this high-pressure apparatus. It was not possible to create fibers at pressures above ~800 psia since DCM was extracted so quickly from the solution that the needle clogged.

Several different processes are operational during the spinning of fibers into CO_2. Figure 2 shows that CO_2 easily dissolves DCM and large amounts of CO_2 dissolve into the DCM-rich liquid phase. At a fixed operating pressure CO_2 dissolves into the PVP−DCM mixture and induces a phase separation, which likely occurs via spinodal decomposition[10] that sets up the initial polymer-rich, liquid network structure. Given that a typical fiber shown in Figure 3 has a radius of ~10 μm, the time for the mass uptake of CO_2 to reach 50% of its final value in a cylindrical, PVP−DCM liquidlike fiber is less than 0.06 s,[13] assuming that the diffusion coefficient for CO_2 (D_{CO_2}) is ~10^{-6} cm^2/s, which is slightly lower than that for a gas diffusing into a liquid. Even with $D_{CO_2} = 10^{-7}$ cm^2/s, CO_2 reaches 50% of its final value in less than 0.6 s.[13] The fiber rapidly develops a skin as DCM is extracted from the surface of the nascent fiber where the plasticizing effect of DCM is diminished, and the effective T_g of PVP quickly surpasses the operating temperature. Simultaneously, CO_2 replaces DCM in the PVP which causes the PVP to swell and also lowers the effective T_g of PVP, although the plasticizing effect of DCM is expected to be greater than that of CO_2.[13−18] A porous, open-cell structure is set up in the interior of the fiber as a result of the large amounts of CO_2 in the PVP−DCM solution and the lowered interfacial tension of the PVP−DCM−CO_2 phase relative to the CO_2−DCM phase. This open-cell structure is frozen in as sufficient amounts of DCM are removed by CO_2 to increase the effective T_g above the operating temperature. Essentially CO_2 acts as a porogen that helps create the interior porous structure although CO_2 has less of an effect on the rapidly formed exterior skin of the fiber, which has a very low concentration of DCM. CO_2 is easily removed from the fiber when the pressure is released at the end of the experiment. The key question for this CO_2-assisted

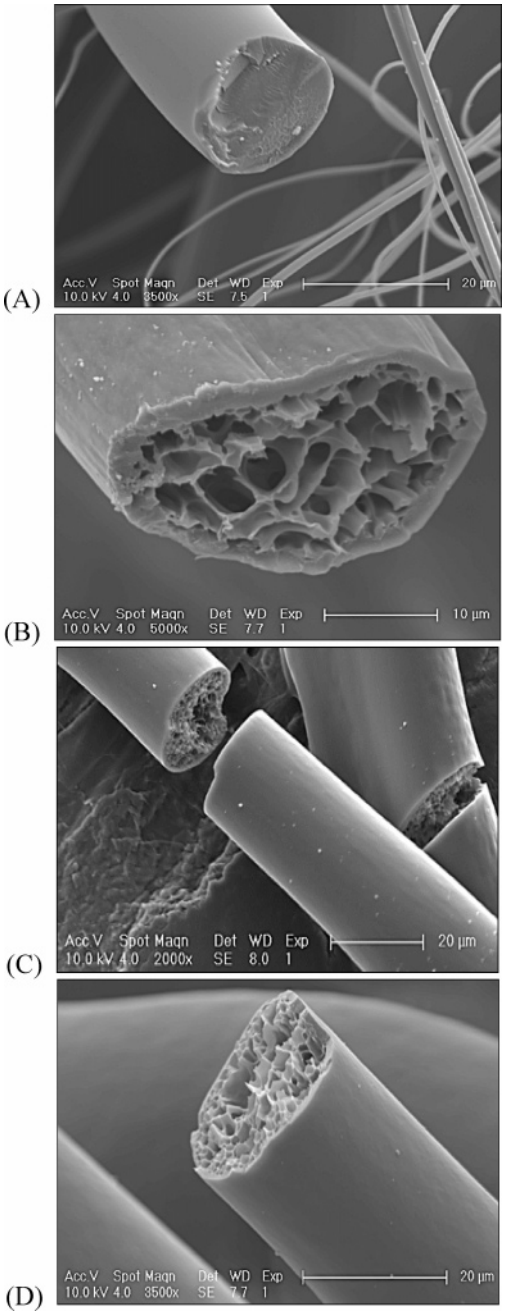

Figure 3. SEM images of the PVP fiber morphologies obtained by spinning into a bath of pure CO_2 at 22 °C and (A) 200, (B) 500, (C) 720, and (D) 740 psia. The voltage potential is set at 20 kV, and the solution delivery rate is the same for all three cases.

electrospinning process is whether the magnitude of the different rates of each of these effects can be tailored to design the internal and external fiber morphologies. A limitation of the beneficial effect of CO_2 is reached at pressures greater than the maximum pressure of the 22 °C isotherm. At this point DCM is miscible with CO_2 in all proportions so that CO_2 readily extracts the DCM out of the solution, which unfortunately causes the solution to clog the needle.

The high-pressure electrospinning cell is currently being redesigned to isolate electrically the charge on the needle from that on the target. With this new design it will be possible to increase the needle to target distance to allow more time for the near-critical fluid to extract the solvent and to create nanofibers. It is important to recognize that extreme pressures are not needed to tailor a specific morphology when using a

near-critical fluid, such as CO_2. The effective removal of the solvent from the polymer solution depends on the partitioning of the liquid solvent between the PVP-rich phase and the CO_2-rich phase. Solubility levels will be fixed by the type of intermolecular interactions between the components in each phase. Further experiments are in progress to demonstrate the impact of the organic solvent used for the polymer solution on the resultant fiber morphology. Also, although not demonstrated here, CO_2 can be loaded into the mixer section of the apparatus to lower the solution viscosity, making it possible to spin normally viscous polymers and polymer solutions.

Acknowledgment. The authors express their appreciation to Diane Gee, Georgio Karles, Joseph Banyasz, Gary Huvard, and Manuel Marquez for helpful technical discussions on electrospinning and Vicki Baliga and Jeffrey Molnar for the SEM analysis. The authors acknowledge Jay Fournier and Peter Lipowicz for the sustained support and guidance they have provided at the Research Center of Philip Morris USA.

References and Notes

(1) Huang, Z.-M.; Zhang, Y.-Z.; Kotaki, M.; Ramakrishna, S. *Compos. Sci. Technol.* **2003**, *63*, 2223−2253.
(2) Li, D.; Xia, Y. *Adv. Mater.* **2004**, *16*, 1151−1170.
(3) Kendall, J. L.; Canelas, D. A.; Young, J. L.; DeSimone, J. M. *Chem. Rev.* **1999**, *99*, 543−563.
(4) Mandel, F. S.; Green, C. D.; Scheibelhoffer, A. S. Method of preparing coating materials. 5,399,597, March 21, 1995.
(5) McHugh, M. A.; Krukonis, V. J. *Supercritical Fluid Extraction: Principles and Practice*, 2nd ed.; Butterworth-Heinemann: Boston, 1994; p 512.
(6) Kazarian, S. G. *J. Polym. Sci., Ser. C* **2000**, *42*, 78−101.
(7) Kikic, I.; Vecchione, F. *Curr. Opin. Solid State Mater. Sci.* **2003**, *7*, 399−405.
(8) Kirby, C. F.; McHugh, M. A. *Chem. Rev.* **1999**, *99*, 565−602.
(9) Meilchen, M. A.; Hasch, B. M.; McHugh, M. A. *Macromolecules* **1991**, *24*, 4874−4882.
(10) Bognitzki, M.; Czado, W.; Frese, T.; Schaper, A.; Hellwig, M.; Steinhart, M.; Greiner, A.; Wendorff, J. H. *Adv. Mater.* **2001**, *13*, 70−72.
(11) Megelski, S.; Stephens, J. S.; Chase, D. B.; Rabolt, J. F. *Macromolecules* **2002**, *35*, 8456−8466.
(12) Tsivintzelis, I.; Missopolinou, D.; Kalogiannis, K.; Panayiotou, C. *Fluid Phase Equilib.* **2004**, *224*, 89−96.
(13) Pantoula, M.; Panayiotou, C. *J. Supercrit. Fluids* **2006**, *37*, 254−262.
(14) Chow, T. S. *Macromolecules* **1980**, *13*, 362−364.
(15) Kalospiros, N. S.; Paulaitis, M. E. *Chem. Eng. Sci.* **1994**, *49*, 659−668.
(16) Smith, P. B.; Moll, D. J. *Macromolecules* **1990**, *23*, 3250−3256.
(17) Wen, W.-Y. *Chem. Soc. Rev.* **1993**, *22*, 117−126.
(18) Wissinger, R. G.; Paulaitis, M. E. *Ind. Eng. Chem. Res.* **1991**, *30*, 842−851.

MA062155I